Available online at www.sciencedirect.com
ScienceDirect
Acta Mathematica Scientia 2012,**32B**(4):1647–1661
Acta Mathematica Scientia 数学物理学报
http://actams.wipm.ac.cn

MUSIC ALGORITHM FOR LOCATING POINT-LIKE SCATTERERS CONTAINED IN A SAMPLE ON FLAT SUBSTRATE*

Dong Heping (董和平)† *Ma Fuming* (马富明) *Zhang Deyue* (张德悦)
Institute of Mathematics, Jilin University, Changchun 130012, China
E-mail: dhp@jlu.edu.cn; mfm@jlu.deu.cn; dyzhang@mail.jlu.edu.cn

Abstract In this paper, we consider a MUSIC algorithm for locating point-like scatterers contained in a sample on flat substrate. Based on an asymptotic expansion of the scattering amplitude proposed by Ammari et al., the reconstruction problem can be reduced to a calculation of Green function corresponding to the background medium. In addition, we use an explicit formulation of Green function in the MUSIC algorithm to simplify the calculation when the cross-section of sample is a half-disc. Numerical experiments are included to demonstrate the feasibility of this method.

Key words MUSIC algorithm; Hemholtz equation; multi static response (MSR) matrix; Green function

2010 MR Subject Classification 78A46

1 Introduction

MUltiple SIgnal Classification (MUSIC) is well known for signal-processing applications. It makes use of the eigenvalue structure of the so-called multistatic response (MSR) matrix generated by an array of transceivers to obtain the positions of the small objects (representing scatterers that are of small size with respect to the wave-length). Since Devaney [1] applied the MUSIC algorithm to the problem of estimating the locations of point-like scatterers in 2000, this method was of great interest in the inverse scattering problems. In [9–11], some numerical methods of MUSIC type for efficiently determining the locations or shapes of a collection of small inclusions in two-dimensional scalar scattering situations were designed, and the methods were extended to full three-dimensional vector electromagnetic in order to retrieve either dielectric inclusions or magnetic inclusions or their combinations [12]. The papers [3, 13, 16] pointed out the strong relation between MUSIC-type algorithms and linear sampling methods. In [20], the MUSIC algorithm was generalized to investigate the influence of the test dipole on the

*Received October 16, 2009; revised August 25, 2011. This work was supported by the National Natural Science Foundation of China (10971083, 10801063) and the School of Mathematical Sciences Foundation of Jilin University.

†Corresponding author: Dong Heping.

resolution of the MUSIC imaging method which was applied to the electromagnetic inverse scattering problem of determining the locations of a collection of small objects embedded in a known background medium. Recently, Park and Lesselier designed a MUSIC-type imaging method for locating thin penetrable inclusion and arc-like cracks in [18, 19], and the paper [25] presented a general framework for imaging perfectly conducting cracks from measurements at single or multiple frequencies. In [22], for the same two-half-space medium as [10], an improved imaging algorithm operated at multiple frequencies was proposed based on a rigorously derived asymptotic expansion formula associated with the presence of a thin dielectric inclusion. In addition, a non-iterative method of MUSIC type was designed in [24] for localizing the corrosive parts from voltage-to-current observations. The authors of [21] developed a direct imaging algorithm for point and extended targets based on a physical factorization of the response matrix of a transducer array. In [26], the problem addressed was to detect and localize a point reflector embedded in a medium by sensor array imaging when the array response matrix is obtained in a noisy environment. Moreover, we would like to refer the readers to [2, 4, 17] about time-reversal-based imaging methods and the decomposition of the time-reversal operator (D.O.R.T.) technique, as well as monograph [14] for a systematic exposition of developments on the reconstruction of small inclusions. For more knowledge of inverse scattering problems see [5, 8, 23].

In this paper, we consider a problem for locating point-like scatterers contained in a sample on flat substrate by using MUSIC algorithm. It is assumed that a penetrable sample containing some point-like scatterers is deposited on an impenetrable substrate, and the sample and the substrate are invariant in one direction. We take a mono-frequency line source to illuminate the sample, and use the scattered field data measured near the sample to estimate the locations of the point-like scatterers. The problem is considered in a plane perpendicular to the invariant direction. Thus, the model problem can be reduced to a two-dimensional case. Based on a asymptotic expansion [9, 10], the reconstruction problem can be reduced to the calculation of Green function corresponding to the background medium. In the numerical experiments, the feasibility of this method was illustrated, even if there is a multiple scattering between the point-like scatterers. In addition, we employ an explicit formulation of Green function in the MUSIC algorithm to simplify the calculation when the cross-section of sample is a half-disc. For some other forms of Green function [27] for Helmholtz equation we refer to [7, 10].

The paper is organized as follows. In Section 2 we describe the model problem in detail, and transform the model problem defined in a half-plane into a new problem defined in the whole plane by symmetric continuation. In Section 3, we give the MUSIC algorithm by using asymptotic expansions. Some numerical examples are shown to demonstrate the effectiveness of this method. In Appendix, we derive an explicit formulation of Green function for Helmholtz equation in a special case.

2 Formulation of Model Problem

Assume that a penetrable sample is deposited on an impenetrable substrate. The sample contains some point-like scatterers, and the substrate is so thick that only upper half-space needs to be considered. It is also assumed that the sample and substrate are invariant along

with direction x_3. The sample is illuminated by a mono-frequency line source parallel to the x_3-axis. Thus, the problems can be reduced to two-dimensional ones. The direct scattering problem is to investigate the scattered field in the upper half-space generated by the sample. The inverse scattering problem then can be formed to locating the set of unknown point-like scatterers in the sample. The geometry of our problem can be described as follows. Let T be a smooth curve in the upper half-plane $\mathbb{R}^2_+ := \{(x_1, x_2) : x_2 > 0\} \subset \mathbb{R}^2$ such that only its two end-points $a = (a_1, 0)$ and $b = (b_1, 0)$ with $a_1 > b_1$ lie on the boundary $\partial\mathbb{R}^2_+$. Then the boundary ∂D of domain D occupied by the section of sample can be written as $\partial D = T \cup \overline{ba}$, where $\overline{ba}$ is the line-segment of two points a and b. Denote $T_- := \{(x_1, 0) : -\infty < x_1 < b_1\}$ and $T_+ := \{(x_1, 0) : a_1 < x_1 < +\infty\}$, and let D_e be the unbounded domain above $\partial D_e := T_- \cup T \cup T_+$. For $x = (x_1, x_2) \in \mathbb{R}^2_+$ denote $x^\rho = (x_1, -x_2)$ which is the reflection of x about the x_1-axis.

Under assumptions similar to [10], the collection of point-like scatterers can be stated as follows. The geometry of each of them may take the form of $C_j + \alpha B_j, j = 1, \cdots, l$, where $C_j = (x_1^j, x_2^j) \in \mathbb{R}^2_+$ determine the locations of the point-like scatterers, B_j's are bounded, smooth domains containing the origin and α denote the common order of magnitude of the diameters of the point-like scatterers. The points C_j, $j = 1, 2, \cdots, l$, satisfy

$$|C_j - C_i| \geq d_0 > 0, \quad \forall j \neq i,$$

and the value of d_0 is large with respect to α. Moreover, we also assume that

$$\min_{1 \leq j \leq l} \{x_2^j\} \geq d_0 > 0.$$

The total collection of point-like scatterers thus takes the form $I_\alpha = \bigcup_{j=1}^{l} (C_j + \alpha B_j)$.

In our problem, the electric permittivity is assumed to be piecewise constant:

$$\varepsilon(x) = \begin{cases} \varepsilon_1, & x \in D_e, \\ \varepsilon_2, & x \in D \backslash \overline{I_\alpha}, \\ \varepsilon_0, & x \in C_j + \alpha B_j, \quad j = 1, \cdots, l. \end{cases}$$

Accordingly, the piecewise positive real-valued wave number k is defined by

$$k(x) := \begin{cases} k_1 = \omega\sqrt{\mu\varepsilon_1}, & x \in D_e, \\ k_2 = \omega\sqrt{\mu\varepsilon_2}, & x \in D \backslash \overline{I_\alpha}, \\ k_0 = \omega\sqrt{\mu\varepsilon_0}, & x \in C_j + \alpha B_j, \quad j = 1, \cdots, l, \end{cases}$$

where ω is the frequency, and μ is the constant magnetic permeability.

Furthermore, let T_1 be a smooth curve in unbounded domain D_e with two end-points $c = (c_1, 0)$ and $d = (d_1, 0)$, such that $c_1 > a_1$ and $b_1 > d_1$. We put a point source $\Phi^i(x, z) = \Phi(x, z)$ at z, $z \in T_1$, as the incident field, where $\Phi(x, z) := \mathrm{i}H_0^{(1)}(k_1|x - z|)/4$ for $x \neq z$ is the fundamental solution of the Helmholtz equation in two-dimensional case, and $H_0^{(1)}$ is the Hankel function of order zero and of the first kind.

The direct scattering problem is to find $w(x,z)=\Phi^i(x,z)+\Phi^\rho(x,z)+w^s_\Phi(x,z)$ satisfying the Helmholtz equation

$$\Delta_x w(x,z)+k^2(x)w(x,z)=0, \qquad x\in\mathbb{R}^2_+, \quad z\in T_1 \tag{2.1}$$

and the Dirichlet boundary condition

$$w(x,z)=0, \qquad x\in\partial\mathbb{R}^2_+, \quad z\in T_1, \tag{2.2}$$

where $\Phi^\rho(x,z)=-\Phi(x,z^\rho)$ is the solution of the scattering problem for the half-plane, i.e., the absence of D. The unknown scattered field $w^s_\Phi(x,z)$ is required to satisfy the Sommerfeld radiation condition

$$\lim_{r\to\infty}\sqrt{r}\left(\frac{\partial w^s_\Phi(x,z)}{\partial r}-\mathrm{i}k_1 w^s_\Phi(x,z)\right)=0, \qquad r=|x|, \quad z\in T_1 \tag{2.3}$$

uniformly for all directions $\hat{x}=\frac{x}{|x|}\in\Omega_+:=\{(x_1,x_2)\in\Omega: x_2\geq 0\}$, where $\Omega:=\{x\in\mathbb{R}^2: |x|=1\}$. The geometry of this model problem is shown in Fig. 1.

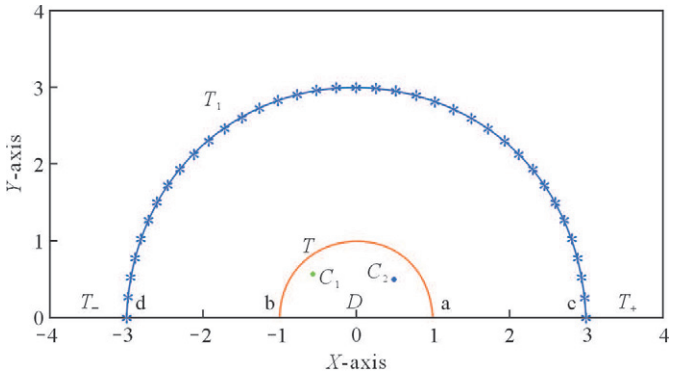

Fig.1 Geometry of the model problem. T_1 and T are the boundaries of measurement (incidence) and sample, respectively; X-axis denotes the substrate; C_1 and C_2 are the centers of point-like scatterers.

The inverse scattering problem can be stated as follows: determine the locations of point-like scatterers $C_j, j=1,\cdots,l$, by use of the near field measurement data $w^s_\Phi(x,z)$ for all $x,z\in T_1$.

Equation (2.1) can be rewritten as

$$\Delta_x w(x,z)+k_1^2 n(x)w(x,z)=0, \qquad x\in\mathbb{R}^2_+, \quad z\in T_1, \tag{2.4}$$

where the wave number $k_1=\omega\sqrt{\mu\varepsilon_1}$, the index of refraction

$$n(x)=\begin{cases}1, & x\in D_e,\\ \varepsilon_2/\varepsilon_1, & x\in D\backslash\overline{I_\alpha},\\ \varepsilon_0/\varepsilon_1, & x\in C_j+\alpha B_j, \quad j=1,\cdots,l.\end{cases}$$

In the following we reformulate the scattering problem (2.4) with conditions (2.2) and (2.3) to one defined in the whole plane. To this end, we denote the mirror image of T, T_1 and I_α about x_1-axis by $T^\rho := \{x^\rho : x \in T\}$, $T_1^\rho := \{x^\rho : x \in T_1\}$ and $I_\alpha^\rho = C_j^\rho + \alpha B_j^\rho, j = 1, \cdots, l$, respectively. Then, we obtain the bounded domain $\widetilde{D}$ closed by boundary $\partial\widetilde{D} = T \cup T^\rho$ and the bounded domain $\widetilde{M}$ closed by boundary $\partial\widetilde{M} = T_1 \cup T_1^\rho$. Furthermore, we assume that $\partial\widetilde{D} \in C^2$ and $\partial\widetilde{M} \in C^2$. Let

$$\widetilde{\varepsilon}(x) = \begin{cases} \varepsilon_1, & x \in \mathbb{R}^2 \backslash \overline{\widetilde{D}}, \\ \varepsilon_2, & x \in \widetilde{D} \backslash \overline{\widetilde{I}_\alpha}, \\ \varepsilon_0, & x \in \widetilde{I}_\alpha \end{cases}$$

and

$$\widetilde{n}(x) = \begin{cases} 1, & x \in \mathbb{R}^2 \backslash \overline{\widetilde{D}}, \\ \varepsilon_2/\varepsilon_1, & x \in \widetilde{D} \backslash \overline{\widetilde{I}_\alpha}, \\ \varepsilon_0/\varepsilon_1, & x \in \widetilde{I}_\alpha. \end{cases}$$

Then problem (2.4) with conditions (2.2) and (2.3) is equivalent to the following problem: find a solution $w(x,z) = \Phi^i(x,z) + \Phi^\rho(x,z) + w_\Phi^s(x,z)$ of the Helmholtz equation

$$\Delta_x w(x,z) + k_1^2 \widetilde{n}(x) w(x,z) = 0, \qquad x \in \mathbb{R}^2, \quad z \in \partial\widetilde{M} \tag{2.5}$$

with the Sommerfeld radiation condition

$$\lim_{r\to\infty} \sqrt{r}\left(\frac{\partial w_\Phi^s(x,z)}{\partial r} - \mathrm{i}k w_\Phi^s(x,z)\right) = 0, \qquad r = |x|, \quad z \in \partial\widetilde{M} \tag{2.6}$$

uniformly for all direction $\hat{x} = x/|x| \in \Omega$. Here inverse scattering problem corresponding to scattering problem in the whole plane can be stated as follows: by use of the near field measurement data $w_\Phi^s(x,z)$, for all $x, z \in \partial\widetilde{M}$, determine the locations of point-like scatterers $C_j \cup C_j^\rho, j = 1, \cdots, l$. For the proof of equivalence between scattering problems in the half-plane and the whole plane, we refer readers to [15] (Theorem 2.1).

3 MUSIC Algorithm and Numerical Implementation

In this section, we design a MUSIC-type algorithm to our model problem and give some numerical results. Since the Green function $g(x,y)$ corresponding to the background medium can be seen as the total field generated by the background medium $\widetilde{D}$ (absence of $\widetilde{I}_\alpha$) with incident field $\Phi^i(x,z)$ [6], we rewrite the problem (2.5)–(2.6) as follows: find $w(x,z) = g^i(x,z) + g^\rho(x,z) + w_g^s(x,z)$, satisfying

$$\Delta_x w(x,z) + k_b^2 m_b(x) w(x,z) = 0, \qquad x \in \mathbb{R}^2, \quad z \in \partial\widetilde{M}, \tag{3.1}$$

$$\lim_{r\to\infty} \sqrt{r}\left(\frac{\partial w_g^s(x,z)}{\partial r} - \mathrm{i}k_1 w_g^s(x,z)\right) = 0, \qquad r = |x|, \quad z \in \partial\widetilde{M}, \tag{3.2}$$

where $g^i(x,z) = g(x,z)$, $g^\rho(x,z) = -g(x,z^\rho)$, wave number

$$k_b(x) = \begin{cases} k_1 = \omega\sqrt{\mu\varepsilon_1}, & x \in \mathbb{R}^2 \backslash \overline{\widetilde{D}}, \\ k_2 = \omega\sqrt{\mu\varepsilon_2}, & x \in \widetilde{D}, \end{cases}$$

and the index of refraction

$$m_b(x) = \begin{cases} 1, & x \in \mathbb{R}^2 \backslash \overline{\widetilde{I}_\alpha}, \\ \varepsilon_0/\varepsilon_2, & x \in \widetilde{I}_\alpha. \end{cases}$$

By the uniqueness of the solution for the problem (2.5)–(2.6), we have that

$$w_\Phi^s = (g^i + g^\rho) - (\Phi^i + \Phi^\rho) + w_g^s = (g_i^s + g_\rho^s) + w_g^s, \tag{3.3}$$

where $g_i^s + g_\rho^s$ is the scattered field generated by the background medium $\widetilde{D}$ (absence of $\widetilde{I}_\alpha$) with incident filed $\Phi^i + \Phi^\rho$. Therefore, to know the scattered field w_Φ^s is equivalent to know w_g^s in the inverse scattering problem.

It is well known that the solution of problem (3.1)–(3.2) satisfies the Lippmann-Schwinger equation

$$\begin{aligned} w(x,z) &= g^i(x,z) + g^\rho(x,z) - \int_{\widetilde{I}_\alpha} k_b^2 g(x,y)(1 - m_b(y))w(y,z)\mathrm{d}y \\ &= g^i(x,z) + g^\rho(x,z) - k_2^2(1 - \frac{\varepsilon_0}{\varepsilon_2}) \int_{I_\alpha \cup I_\alpha^\rho} g(x,y)w(y,z)\mathrm{d}y. \end{aligned} \tag{3.4}$$

By arguments similar to those in [10], we have that

$$\int_{C_j + \alpha B_j} g(x,y)w(y,z)\mathrm{d}y = g(x,C_j) \int_{C_j + \alpha B_j} w(y,z)\mathrm{d}y + o(\alpha^2), \tag{3.5}$$

$$\int_{C_j + \alpha B_j} w(y,z)\mathrm{d}y = \alpha^2 |B_j| \Big(g^i(C_j,z) + g^\rho(C_j,z) \Big) + o(\alpha^2), \tag{3.6}$$

$j = 1, \cdots, 2l$, where $C_{l+i} = C_i^\rho$, $B_{l+i} = B_i^\rho, i = 1, \cdots, l$, $\tau_j = k_2^2(\varepsilon_0/\varepsilon_2 - 1)\alpha^2|B_j|$, $\tau_{l+i} = \tau_i$. Replacing (3.5) and (3.6) into (3.4) with ignoring $o(\alpha^2)$, we get that

$$w_g^s(x,z) \approx \sum_{j=1}^{2l} g(x,C_j)\tau_j \Big(g(C_j,z) - g(C_j,z^\rho) \Big). \tag{3.7}$$

From the symmetry of $\widetilde{D}$ and symmetric continuation, we have that

$$w_\Phi^s(x,z^\rho) = -w_\Phi^s(x,z), \quad w_\Phi^s(x^\rho,z) = -w_\Phi^s(x,z),$$

$$g_i^s(x,z^\rho) = -g_i^s(x,z), \quad g_i^s(x^\rho,z) = -g_i^s(x,z).$$

By (3.3), we obtain

$$w_g^s(x,z^\rho) = -w_g^s(x,z), \quad w_g^s(x^\rho,z) = -w_g^s(x,z).$$

Then,

$$\begin{aligned} 2w_g^s(x,z) &= w_g^s(x,z) - w_g^s(x^\rho,z) \\ &\approx \sum_{j=1}^{2l} \Big(g(x,C_j) - g(x^\rho,C_j) \Big)\tau_j \Big(g(C_j,z) - g(C_j,z^\rho) \Big). \end{aligned}$$

By using reciprocity relation of the Green function, we have that

$$w_g^s(x,z) \approx \sum_{j=1}^{2l} \Big(g(x,C_j) - g(x^\rho,C_j)\Big)\widetilde{\tau}_j \Big(g(z,C_j) - g(z^\rho,C_j)\Big),$$

where $\widetilde{\tau}_j = \tau_j k_2^2/2k_1^2$, so $\widetilde{\tau}_{l+i} = \widetilde{\tau}_i, i = 1,\cdots,l$.

For $x, z \in \partial\widetilde{M}$, we introduce the MSR (multistatic response) matrix

$$\begin{aligned} W_{pm}^s &= \sum_{j=1}^{2l} \Big(g(z_p,C_j) - g(z_p^\rho,C_j)\Big)\widetilde{\tau}_j \Big(g(z_m,C_j) - g(z_m^\rho,C_j)\Big) \\ &\approx w_g^s(x_p,z_m)\,\big|_{x_p=z_p}\,, \end{aligned} \tag{3.8}$$

$p, m = 1,\cdots,2n$ and define $F = \mathrm{diag}(\widetilde{\tau}_1,\cdots,\widetilde{\tau}_{2l}) \in \mathbb{R}^{2l\times 2l}$, $S = [S_1,\cdots,S_{2l}] \in \mathbb{C}^{2n\times 2l}$, and

$$S_j = \Big(g(z_1,C_j) - g(z_1^\rho,C_j),\cdots,g(z_{2n},C_j) - g(z_{2n}^\rho,C_j)\Big)^\top.$$

Since $C_{l+i} = C_i^\rho, i = 1,\cdots,l$, we know $S_{l+i} = -S_i, i = 1,\cdots,l$. Setting $S = [S_0, -S_0]$, where $S_0 = [S_1,\cdots,S_l] \in \mathbb{C}^{2n\times l}$, and $F_0 = \mathrm{diag}(\widetilde{\tau}_1,\cdots,\widetilde{\tau}_l) \in \mathbb{R}^{l\times l}$, we then observe that W^s admits the following decomposition:

$$W^s = SFS^\top = 2S_0F_0S_0^\top. \tag{3.9}$$

It's readily to see that W^s is symmetric and $\overline{W^s}^\top = \overline{W^s}$. If $n \geq l$ and the matrix S_0 has maximal rank l, then the ranges $\mathcal{R}(S_0)$ and $\mathcal{R}(W^s\overline{W^s})$ coincide. Thus,

$$\mathcal{R}(W^s\overline{W^s}) = \mathcal{R}(S_0) = \mathrm{span}\{S_1,\cdots,S_l\}.$$

For any point $C \in \widetilde{D}$, we define vector $f_C \in \mathbb{C}^{2n}$ by

$$f_C = \Big(g(z_1,C) - g(z_1^\rho,C),\cdots,g(z_{2n},C) - g(z_{2n}^\rho,C)\Big)^\top. \tag{3.10}$$

It can be seen that $f_{C_1},\cdots,f_{C_l}$ are the columns of the matrix S_0. Now according to [3], we can show the main tool for the identification of the locations C_j $(j = 1,\cdots,l)$.

Proposition 1 There exists $n_0 \in \mathbb{N}$ such that for any $n \geq n_0$, the following characterization holds

$$f_C \in \mathcal{R}(S_0) \Longleftrightarrow C \in \{C_1,\cdots,C_l\}. \tag{3.11}$$

Since the matrix W^s is symmetric, following [10], the singular value decomposition of the matrix W^s can be defined by $W^s = V\Sigma V^\top$, where $V \in \mathbb{C}^{2n\times 2n}$ is unitary and $\Sigma = \mathrm{diag}\{\sigma_1,\sigma_2,\cdots,\sigma_{2n}\}$ is a real nonegative diagonal matrix, $\sigma_1 \geq \sigma_2 \geq \cdots \geq \sigma_l > 0$, and $\sigma_i = 0, i = l+1,\cdots,2n$. Denote the first l columns of V, $\{v_1,v_2,\cdots,v_l\}$ by V_S, which provide a basis for the space of $\mathcal{R}(W^s)$ and $\{v_{l+1},v_{l+2},\cdots,v_{2n}\}$, the rest of the matrix V, denoted by V_N provides a basis for the left null space of W^s. Then, the best rank approximation for W^s is $V_s\overline{V_s}^\top W^s$.

From Proposition 1, a test-point C coincides with one of the positions $C_j, j = 1,\cdots,l$ if and only if $Pf_C = 0$, where $P = I - V_S\overline{V_S}^\top$ is the orthogonal projection onto the null space of W^s. Thus, we can form an image of $C_j, j = 1,\cdots,l$, by plotting the quantity

$$W(C) = \frac{1}{\|Pf_C\|} \tag{3.12}$$

at each point of C. The resulting plot will have large peaks at the positions $C_j, j = 1, \cdots, l$.

In the numerical experiments presented in this section, the data are generated from numerical computation of direct scattering problems by using of boundary integral equation method. We compute the solution w^s_Φ of direct scattering problem (2.5)–(2.6) and the scattered field w^s_B generated by the background medium $\widetilde{D}$ (absence of $\widetilde{I}_\alpha$) with incident filed $\Phi^i + \Phi^\rho$ respectively. The measurements of scattered field $w^s = w^s_\Phi - w^s_B$, generated by the point-like scatterers, are performed at the set of n incidences in numerical simulation. We make use of MSR matrix $W^s_{pm} = w^s(x_p, z_m)\,|_{x_p=z_p}$, $x, z \in \partial\widetilde{M}$, $p, m = 1, \cdots, 2n$, to locate the point-like scatterers. Noting that there is a significant multiple scattering among the point-like scatterers in this case. However, we find that the MUSIC algorithm behaves in feasible manner.

In the following two examples, we assume that sample D contains two small homogeneous disks with diameter $\alpha = 0.02$, denoted by I_0 and I_1, respectively. We choose $\omega = 1, \mu = 1, \varepsilon_0 = 36, \varepsilon_1 = 1, \varepsilon_2 = 9$, and sampling step $h = 0.02$ in both directions. Thus, the wave numbers are $k_0 = 6$, $k_1 = 1$, $k_2 = 3$.

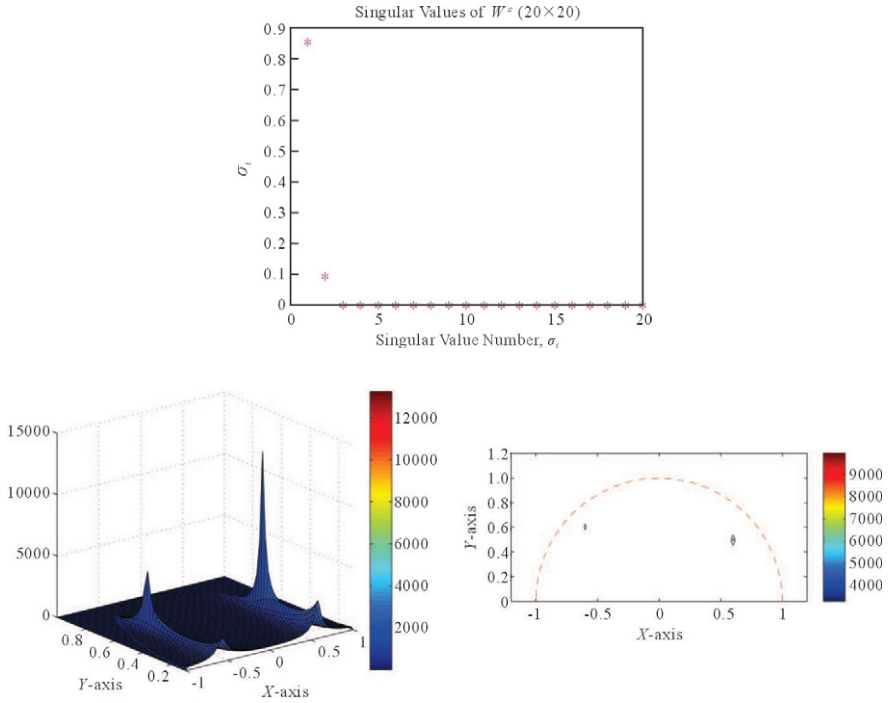

Fig.2 $n = 10$, singular values of W^s, 3D-plot and contour map of $W(C)$ of Example 1

Example 1 In this example, we consider a specific case in which the shape of sample D is a semidisc with radius $r = 1$. The two point-like scatterers are centered at $C_1 = (-0.6, 0.6)$ and $C_2 = (0.6, 0.5)$, and the scattered field $w^s = w^s_\Phi - w^s_B$ is measured at a semicircle ∂M with radius $R = 2$. We take sampling points within a squared box prescribed as

$$\Omega = [-1, 1] \times [0.1, 1].$$

Since we are only interested in the sampling points in sample D, let $W(C) = 0, C \notin \Omega \cap D$. In order to simplify calculations of f_C, an exact formula of Green function g is constructed (see

Appendix). Because of the symmetry of this problem, we only need to put sampling points in the upper half-plane. Fig. 2 and Fig. 3 show the singular values of W^s, 3D-plot and contour map of $W(C)$ when illuminations $n = 10$ and $n = 20$, respectively. It can be seen that the locations of pointer-like scatterers can be reconstructed very well. We also consider the stability of our method for the measurements with noise. The singular values of W^s and 3D-plot of $W(C)$ are displayed in Fig. 4 when the measurements (MSR matrix) generated from boundary integral equation method are perturbed by 0.1% random noises for $n = 10$ (left) and $n = 20$ (right), respectively. Here, the scatterers cannot be still recognized well in the present experiment.

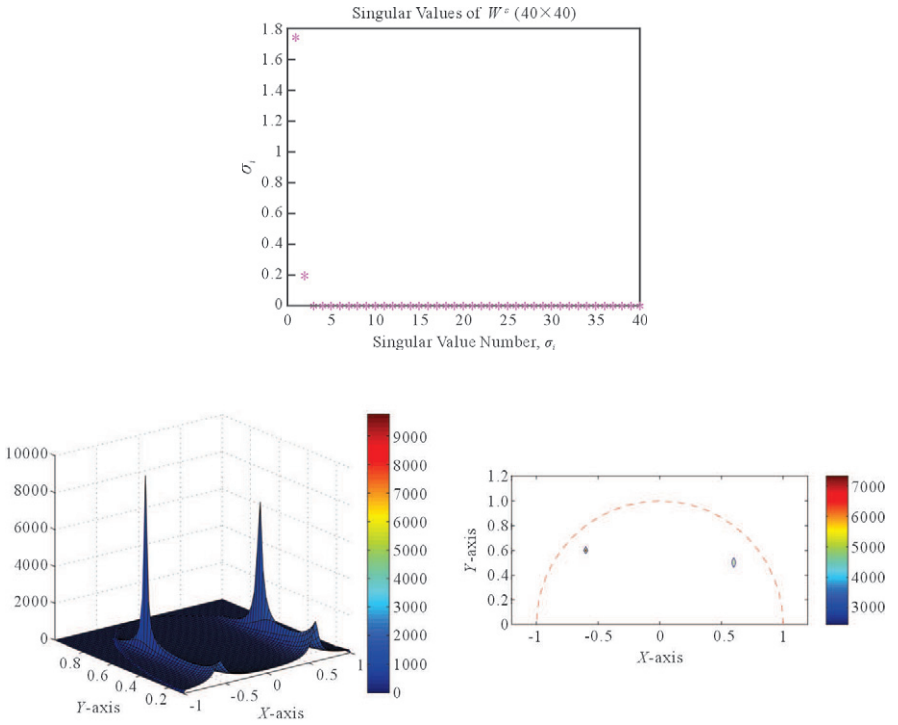

Fig.3 $n = 20$, singular values of W^s, 3D-plot and contour map of $W(C)$ of Example 1

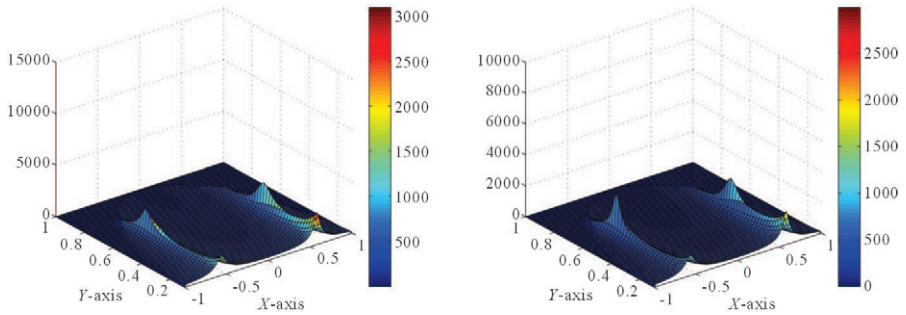

Fig.4 0.1% noise of MSR matrix, $n = 10$ (left), $n = 20$ (right)

Example 2 Now, we take the sample D with a peanut-shape boundary ∂D described

by

$$x(t) = (\cos t\sqrt{4\cos^2 t + \sin^2 t}, \sin t\sqrt{4\cos^2 t + \sin^2 t}), \qquad 0 \le t \le \pi.$$

Analogously, we assume that the sample contains two point-like scatterers, centered at $C_1 = (-1.25, 0.8)$ and $C_2 = (1.1, 0.7)$, respectively. We choose the radius of measurement boundary $R = 3$ and sampling domain $\Omega = [-2, 2] \times [0.1, 1.5]$. In this case, the Green function g in (3.10) is unknown. However, we may give a numerical Green function by solving a direct scattering problem through the boundary integral equation method. It means that we have to compute $g(x, y_0)(y_0 \in \widetilde{D})$ satisfying

$$\begin{aligned}
&\Delta_x g(x, y_0) + k_b^2(x) g(x, y_0) = \delta(|x - y_0|), \qquad x \in \mathbb{R}^2,\\
&g(x, y_0) = \Phi_b(x, y_0) + g^s(x, y_0),\\
&g^s(x, y_0) \ \text{ is bounded in } \mathbb{R}^2,
\end{aligned}$$

where wave number

$$k_b(x) = \begin{cases} k_1 = \omega\sqrt{\mu\varepsilon_1}, & x \in \mathbb{R}^2 \backslash \overline{\widetilde{D}},\\ k_2 = \omega\sqrt{\mu\varepsilon_2}, & x \in \widetilde{D}, \end{cases}$$

incident field $\Phi_b(x, y_0) = \mathrm{i}H_0^{(1)}(k_b(y_0)|x - y_0|)/4$, $g^s(x, y_0)$ and $g(x, y_0)$ denote the scattered field and total field respectively. With help of this Green function, we can compute $W(C)$ like Example 1. Fig. 5 and Fig. 6 show the singular values of W^s, 3D-plot and contour map of $W(C)$ when illuminations $n = 10$ and $n = 20$, respectively. The singular values of W^s and 3D-plot of $W(C)$ are displayed in Fig. 7 when the measurements (MSR matrix) are perturbed by 0.1% random noise, for $n = 10$ (left) and $n = 20$ (right), respectively.

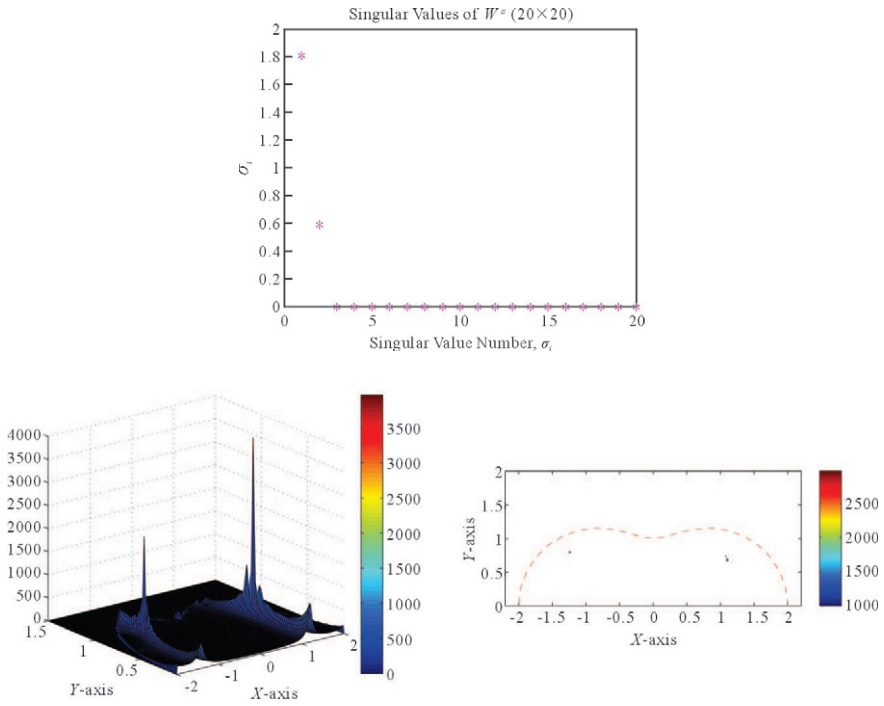

Fig.5 $n = 10$, singular values of W^s, 3D-plot and contour map of $W(C)$ of Example 2

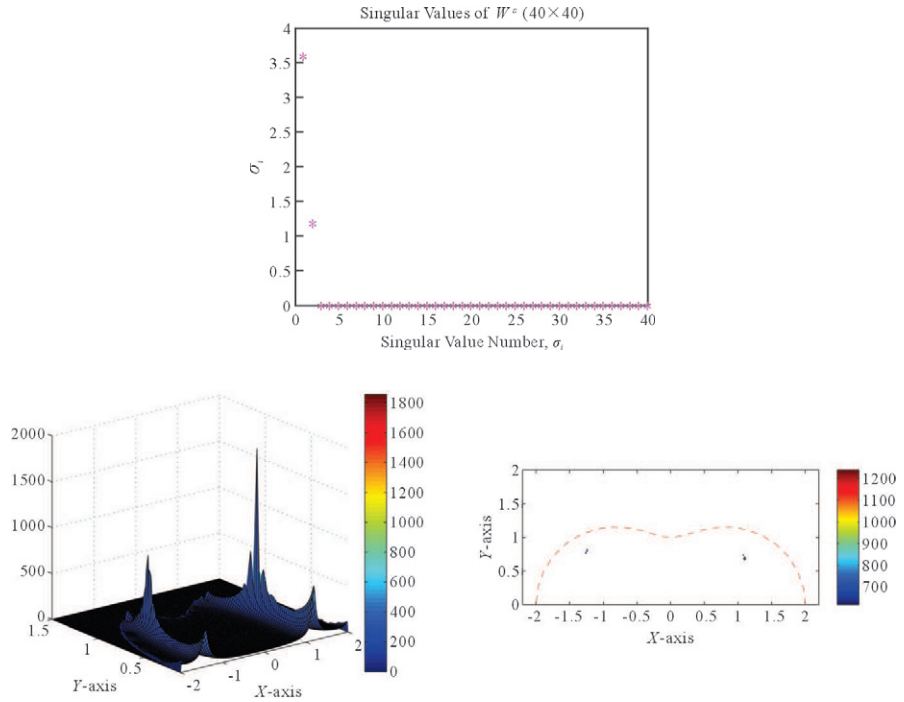

Fig.6 $n = 20$, singular values of W^s, 3D-plot and contour map of $W(C)$ of Example 2

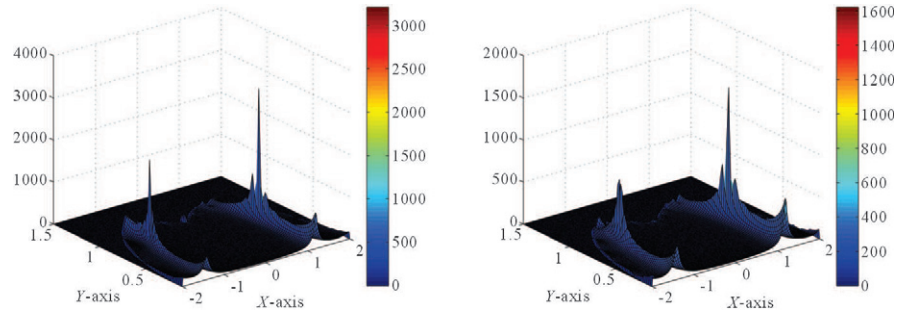

Fig.7 0.1% noise of MSR matrix, $n = 10$ (left), $n = 20$ (right)

4 Conclusion

In this paper, a MUSIC algorithm for locating point-like scatterers contained in a sample on flat substrate has been proposed, and the numerical examples are given to demonstrate the effectiveness of the method. However, the algorithm still has some limitations. Noting that

$$f_C = \Big(g(z_1, C) - g(z_1^\rho, C), \cdots, g(z_{2n}, C) - g(z_{2n}^\rho, C)\Big)^\top,$$

$f_C \equiv 0$ if test point C lies on the x-axis. It means that we are unable to detect the point-like scatterers near x-axis since the value of $W(C) = \frac{1}{\|P f_C\|}$ is extraordinary large whatever the point C coincides with one of the positions C_j or not. In addition, we have added 0.1% noise to

the MSR matrix in our numerical examples, but 0.1% noise is too small in practical application. We will continue to study and try to improve this method in our future research.

References

[1] Devaney A J. Super-resolution processing of multi-static data using time reversal and MUSIC. http://www.ece.neu.edu/faculty/devaney/ajd/preprints.htm

[2] Devaney A J, Marengo E A, Gruber F K. Time-reversal-based imaging and inverse scattering of multiply scattering point targets. J Acoust Soc Am, 2005, **118**: 3129–3138

[3] Kirsch A. The MUSIC algorithm and the factorization method in inverse scattering theory for inhomogeneous media. Inverse Problems, 2002, **18**: 1025–1040

[4] Prada C, Manneville S, Spoliansky D, Fink M. Decomposition of the time reversal operator: Detection and selective focusing on two scatterers. J Acoust Soc Am, 1996, **99**: 2067–2076

[5] Colton D, Kress R. Inverse Acoustic and Electromagnetic Scattering Theory. 2nd ed. Berlin: Springer, 1998

[6] Colton D, Monk P. A linear sampling method for the detection of leukemia using microwaves. SIAM J Appl Math, 1998, **58**: 926–941

[7] Duffy D G. Green's Functions with Applications. Chapman & Hall/CRC, 2001

[8] Cakoni F, Colton D. Qualitative Methods in Inverse Scattering Theory. Berlin: Springer, 2006

[9] Ammari H, Iakovleva E, Moskow S. Recovery of small inhomogeneities from the scattering amplitude at a fixed frequency. SIAM J Math Anal, 2003, **34**: 882–900

[10] Ammari H, Iakovleva E, Lesselier D. A MUSIC algorithm for locating small inclusions buried in a half-space from the scattering amplitude at a fixed frequency. Multiscale Model Simul, 2005, **3**: 597–628

[11] Ammari H, Iakovleva E, Lesselier D. Two numerical methods for recovering small inclusions from the scattering amplitude at a fixed frequency. SIAM J Sci Comput, 2005, **27**: 130–158

[12] Ammari H, Iakovleva E, Lesselier D, Perruson G. MUSIC-type electromagnetic imaging of a collection of small three-dimensional bounded inclusions. SIAM J Sci Comput, 2007, **29**: 674–709

[13] Ammari H, Griesmaier R, Hanke M. Identification of small inhomogeneities: Asymptotic factorization. Math Comput, 2007, **76**: 1425–1448

[14] Ammari H, Kang H. Reconstruction of Small Inhomogeneities from Boundary Measurements. Berlin: Springer, 2004

[15] Dong H P, Ma F M. Reconstruction of the shape of object with near field measurements in a half-plane. Science in China Series A: Mathematics, 2008, **51**: 1059–1070

[16] Cheney M. The linear sampling method and the MUSIC algorithm. Inverse Problems, 2001, **17**: 591–595

[17] Fink M, Prada C. Acoustic time-reversal mirrors. Inverse Problems, 2001, **17**: R1–R38

[18] Park W K, Lesselier D. MUSIC-type imaging of a thin penetrable inclusion from its multi-static response matrix. Inverse Problems, 2009, **25**: 075002

[19] Park W K, Lesselier D. Electromagnetic MUSIC-Type Imaging of Perfectly Conducting, Arc-Like Cracks at Single Frequency. Journal of Computational Physics, 2009, **228**(21): 8093–8111

[20] Chen X D, Zhong Y. MUSIC electromagnetic imaging with enhanced resolution for small inclusions. Inverse Problems, 2009, **25**: 015008

[21] Hou S, Huang K, Sølna K, Zhao H. A phase and space coherent direct imaging method. J Acoust Soc Am, 2009, **125**: 227–238

[22] Park W K. On the imaging of thin dielectric inclusions buried within a half-space. Inverse Problems, 2010, **26**: 074008

[23] Ammari H. An Introduction to Mathematics of Emerging Biomedical Imaging. Mathematics and Applications, Volume 62. Berlin: Springer, 2008

[24] Ammari H, Kang H, Kim E, Louati K, Vogelius M. A MUSIC-type algorithm for detecting internal corrosion from electrostatic boundary measurements. Numerische Mathematik, 2008, **108**: 501–528

[25] Ammari H, Garnier J, Kang H, Park W K, Sølna K. Imaging schemes for perfectly conducting cracks. SIAM J Appl Math, 2011, **71**: 68–91

[26] Ammari H, Garnier J, Sølna K. A statistical approach to optimal target detection and localization in the presence of noise. Waves in Random and Complex Media, 2012, **22**(1): 40–65

[27] Liu Taiping, Zeng Yanni. On Green's function for hyperbolic-parabolic systems. Acta Mathematica Scientia, 2009, **29**(6): 1556–1572

Appendix Construction of Green Function

In this Appendix, we derive an exact formula of Green function for special scattering problem of Helmholtz equation.

Let us denote the Green function $g(r,\theta|\rho,\theta')$ governed by the planar Helmholtz equation in terms of polar coordinates

$$\frac{1}{r}\frac{\partial}{\partial r}(r\frac{\partial g}{\partial r})+\frac{1}{r^2}\frac{\partial^2 g}{\partial\theta^2}+k_b^2 g=-\frac{\delta(r-\rho)\delta(\theta-\theta')}{r}, \tag{A.1}$$

where $0<r,\rho<\infty$, $0\le\theta,\theta'\le 2\pi$ with the interface condition

$$\big[g\big]=\Big[\frac{1}{\varepsilon_b}\frac{\partial g}{\partial r}\Big]=0, \qquad r=a, \tag{A.2}$$

and condition

$$\lim_{r\to\infty}|g(r,\theta|\rho,\theta')|<\infty. \tag{A.3}$$

Here

$$k_b(x)=\begin{cases}k_1=\omega\sqrt{\mu\varepsilon_1}, & x\in\mathbb{R}^2\backslash\overline{B_a},\\ k_2=\omega\sqrt{\mu\varepsilon_2}, & x\in B_a,\end{cases}$$

$$\varepsilon_b(x)=\begin{cases}\varepsilon_1, & x\in\mathbb{R}^2\backslash\overline{B_a},\\ \varepsilon_2, & x\in B_a,\end{cases}$$

where $B_a:=\{x\in\mathbb{R}^2:|x|<a\}$, ω is the frequency, and μ is the magnetic permeability.

From [7], we have that

$$\delta(\theta-\theta')=\frac{1}{2\pi}+\frac{1}{\pi}\sum_{n=1}^{\infty}\cos[n(\theta-\theta')]=\frac{1}{2\pi}\sum_{n=-\infty}^{+\infty}\cos[n(\theta-\theta')], \tag{A.4}$$

so that the solution g can be of the form

$$g(r,\theta|\rho,\theta')=\sum_{n=-\infty}^{+\infty}g_n(r,\rho)\cos[n(\theta-\theta')]. \tag{A.5}$$

Substituting (A.4) and (A.5) into (A.1), we find that

$$\frac{1}{r}\frac{\partial}{\partial r}\left(r\frac{\partial g_n}{\partial r}\right)-\frac{n^2}{r^2}g_n+k_b^2 g_n=-\frac{\delta(r-\rho)}{2\pi r}, \tag{A.6}$$

When $\rho<a$, the homogeneous solution of (A.6) is

$$g_n(r,\rho)=\begin{cases}A_n J_n(k_2 r), & 0\le r\le\rho,\\ B_n J_n(k_2 r)+C_n H_n^{(1)}(k_2 r), & \rho\le r\le a,\\ D_n H_n^{(1)}(k_1 r), & a\le r<+\infty.\end{cases}$$

Here A_n, B_n, C_n, D_n are coefficients to be determined, J_n is the Bessel function of first kind of order n, and $H_n^{(1)}$ denotes the Hankel function of first kind of order n. This solution possesses the properties of remaining finite as $r \to 0$ and corresponding to a radiating wave solution in the limit as $r \to \infty$.

Now, by use of the requirements that the solution is continuous at $r = \rho$ and that

$$\rho \frac{\partial g_n}{\partial r}\bigg|_{r=\rho^-}^{r=\rho^+} = -\frac{1}{2\pi},$$

we get that

$$\begin{aligned}
&A_n J_n(k_2\rho) = B_n J_n(k_2\rho) + C_n H_n^{(1)}(k_2\rho),\\
&B_n J_n'(k_2\rho) + C_n H_n^{(1)'}(k_2\rho) - A_n J_n'(k_2\rho) = -\frac{1}{2\pi k_2\rho},\\
&B_n J_n(k_2 a) + C_n H_n^{(1)}(k_2 a) = D_n H_n^{(1)}(k_1 a),\\
&k_1 B_n J_n'(k_2 a) + k_1 C_n H_n^{(1)'}(k_2 a) = k_2 D_n H_n^{(1)'}(k_1 a).
\end{aligned}$$

Since the Wronskian determinant is

$$\begin{aligned}
W[J_n(k_2\rho), H_n^{(1)}(k_2\rho)] &= J_n(k_2\rho)(H_n^{(1)})'(k_2\rho) - J_n'(k_2\rho)H_n^{(1)}(k_2\rho)\\
&= \frac{2\mathrm{i}}{\pi k_2\rho},
\end{aligned} \tag{A.7}$$

we obtain that

$$\begin{aligned}
&C_n = \frac{\mathrm{i}}{4} J_n(k_2\rho),\\
&D_n = \widetilde{D}_n(a) J_n(k_2\rho), \qquad \widetilde{D}_n(a) = \frac{k_1}{k_2}\cdot\frac{1}{2\pi a T_n(a)},\\
&B_n = \widetilde{B}_n(a) J_n(k_2\rho), \qquad \widetilde{B}_n(a) = \frac{\widetilde{D}_n(a) H_n^{(1)}(k_1 a) - \frac{\mathrm{i}}{4} H_n^{(1)}(k_2 a)}{J_n(k_2 a)},\\
&A_n = \widetilde{B}_n(a) J_n(k_2\rho) + \frac{\mathrm{i}}{4} H_n^{(1)}(k_2\rho),
\end{aligned}$$

where $T_n(a) = k_1 H_n^{(1)}(k_1 a) J_n'(k_2 a) - k_2 (H_n^{(1)})'(k_1 a) J_n(k_2 a)$.

The case $\rho > a$ can be solved analogously to $\rho < a$. Therefore, the Green function is

- $\rho < a$, $r \le a$,

$$\begin{aligned}
g(r,\theta|\rho,\theta') = 2\sum_{n=1}^{\infty} &\left\{ \widetilde{B}_n(a) J_n(k_2 r_>) J_n(k_2 r_<) + \frac{\mathrm{i}}{4} H_n^{(1)}(k_2 r_>) J_n(k_2 r_<) \right\}\\
&\cdot \cos[n(\theta - \theta')] + \left\{ \widetilde{B}_0(a) J_0(k_2 r_>) J_0(k_2 r_<) + \frac{\mathrm{i}}{4} H_0^{(1)}(k_2 r_>) J_0(k_2 r_<) \right\},
\end{aligned}$$

- $\rho < a$, $r > a$,

$$g(r,\theta|\rho,\theta') = 2\sum_{n=1}^{\infty} \left\{ \widetilde{D}_n(a) J_n(k_2\rho) H_n^{(1)}(k_1 r) \right\} \cos[n(\theta - \theta')] + \widetilde{D}_0(a) J_0(k_2\rho) H_0^{(1)}(k_1 r),$$

- $\rho > a$, $r \le a$,

$$g(r,\theta|\rho,\theta') = 2\sum_{n=1}^{\infty} \left\{ \widetilde{a}_n(a) J_n(k_2 r) H_n^{(1)}(k_1\rho) \right\} \cos[n(\theta - \theta')] + \widetilde{a}_0(a) J_0(k_2 r) H_0^{(1)}(k_1\rho),$$

- $\rho > a$, $r > a$,

$$g(r,\theta|\rho,\theta') = 2\sum_{n=1}^{\infty}\left\{\widetilde{c}_n(a)H_n^{(1)}(k_1r_>)H_n^{(1)}(k_1r_<) + \frac{\mathrm{i}}{4}H_n^{(1)}(k_1r_>)J_n(k_1r_<)\right\}$$
$$\cdot\cos[n(\theta-\theta')] + \left\{\widetilde{c}_0(a)H_0^{(1)}(k_1r_>)H_0^{(1)}(k_1r_<) + \frac{\mathrm{i}}{4}H_0^{(1)}(k_1r_>)J_0(k_1r_<)\right\},$$

where $r_< = \min(r,\rho)$, $r_> = \max(r,\rho)$, and

$$\widetilde{a}_n(a) = \frac{k_2}{k_1}\cdot\frac{1}{2\pi aT_n(a)},$$
$$\widetilde{c}_n(a) = \frac{\widetilde{a}_n(a)J_n(k_2a) - \frac{\mathrm{i}}{4}J_n(k_1a)}{H_n^{(1)}(k_1a)}.$$

Note that

$$k_1^2 g_n(r,\rho) = k_2^2 g_n(\rho,r), \qquad r < a, \quad \rho > a$$

and

$$g_n(r,\rho) = g_n(\rho,r), \qquad r,\rho < a \ \text{ or } \ r,\rho > a.$$

Green function $g(x,y)$ satisfies the following reciprocity relation

$$k_1^2 g(x,y) = k_2^2 g(y,x), \qquad x \in B_a, \quad y \in \mathbb{R}^2\backslash\overline{B_a}$$

and

$$g(x,y) = g(y,x), \qquad x,y \in B_a \ \text{ or } \ x,y \in \mathbb{R}^2\backslash\overline{B_a}.$$